DETACHED EDDY SIMULATIONS OF SUPERSONIC FLOW OVER CAVITY

A. Hamed*, D. Basu**, K. Das**
Department of Aerospace Engineering and Engineering Mechanics
University of Cincinnati
Cincinnati, OH 45221-0070

Abstract

Detached Eddy Simulations are performed for unsteady three-dimensional supersonic turbulent flow over an open L/D = 5 cavity at free-stream Mach number of 1.19. Numerical results are obtained from the explicit solution and Shear-Stress-Transport based simulations using the 3rd order Roe scheme. Computational results are presented for the unsteady vortex and shock structures. The acoustic response of the cavity is presented in the form of pressure fluctuations and sound pressure level spectra. The computational results are compared to existing experimental data and to results obtained from two-dimensional Reynolds Averaged Navier Stokes with algebraic turbulence model.

Introduction

Numerical investigations of flow over open cavities based on time dependent Reynolds Averaged Navier-Stokes (URANS) simulations have failed in general to capture the flow unsteadiness[1,2,3], and in some cases the solution even became steady[4]. This was attributed to excessive turbulent dissipation in the used turbulence models. Most of these models were developed for steady flows and much less complicated environment. In particular, URANS simulations did not capture the acoustic turbulence coupling effects, which are important in open cavities.

Direct Numerical Simulations (DNS) offer a mean for resolving the range of length scales in turbulent flow without recourse to conventional turbulence models. However, its computational resources requirement has limited it's application to low Reynolds numbers and laminar or transitional boundary layer[5,6] in 2-D cavities. Colonius et al.[5], used a sixth order compact difference scheme to study subsonic flow over two-dimensional cavities.

The study demonstrated the change from the shear layer mode to the wake mode as the Mach number and cavity length to depth ratio increased. Hamed et al.[6] used a sixth-order compact scheme in conjunction with tenth order implicit filter and Beam-Warming implicit time integration to study unsteady flow over two-dimensional cavity. They predicted a dramatic increase in pressure fluctuations amplitude and sound pressure level at supersonic conditions. The computational resources requirement restricted both studies to low Reynolds number.

Large Eddy Simulations (LES) model the small-scale isotropic turbulence below the smallest grid size while simulating the larger length scales. Rizzetta et al.[7] simulated a supersonic L/D = 5 cavity flow field using LES at a Reynolds number of 0.12_10^6/ft. They used a fourth order spatially compact scheme with tenth order compact filters, and an implicit second order time-accurate method for temporal advancement. The predicted SPL spectra were compared with experimental results[8], obtained at a Reynolds number of 1.86_10^6/ft. The computation, which involved $21x10^6$ grid points, was performed in a parallel computing platform of IBM SP3 with 254 processors.

Sinha et al.[4] performed VLES (Very Large Eddy Simulations), but only for a 2-D cavity flow field, and compared the solutions with URANS predictions using the Baldwin-Lomax turbulence model. The VLES results for SPL spectra at the cavity floor exhibited broadband turbulence that was absent in the URANS results, which only exhibited the principal acoustic tones and the higher harmonics. Sinha et al.[9] subsequently applied a hybrid RANS-LES method to cavity flow fields simulations. Their methodology was based on a combination of one-equation LES model and k-_ RANS model such that RANS solutions are recovered in coarse mesh and LES type solutions in finer mesh regions[4,9].

The inception of Detached eddy Simulations (DES)[10] was motivated by the need to extend the LES capabilities of resolving turbulence in the shear layers and separated flow regions to flows at realistic Reynolds numbers. This was achieved using a single turbulence model, to function as a sub-grid scale model in the LES regions and as one equation[11]

*Professor, AIAA Fellow

**Graduate Student, Student Member AIAA

turbulence model in attached boundary layers RANS solutions. DES has since been applied to a variety of problems such as flow over an airfoil[12], subsonic flow over cavity[13], cylinder[14], surface mounted cube[15], and more recently for the flow over F-15E[16]. In all these simulations the Spalart-Allamaras[11] (S-A) one equation model was used as originally proposed by Spalart et al.[10]. Subsequently, Bush et al.[17] implemented SST[18] based DES model through the introduction of an equivalent length scale, that depends on the grid size and /or distance from wall. They conducted SST based DES for flow over backward facing step, flow over airfoil, and lifting jet flows. The DES simulations yielded finer flow structures compared to URANS on the same grid. Strelets[19] discussed many of the issues involved in DES simulations and presented computational results that demonstrated remarkable improvements in the predictions of the pre and post stall average lift and drag coefficients.

The goal of the present work is to assess the capability of DES in predicting cavity flow fields that involves not only unsteadiness but also complex interactions between acoustics, turbulence and shock waves. The computations were performed using the WIND[20] code with SST based DES model. The study was conducted at the same flow conditions as that of Rizzetta's LES investigation[7], but, with a resolution equivalent to a RANS grid. The present computations involved 0.8×10^6 grid points compared to the 21×10^6 grid points used by Rizzetta et al[7] at the same Reynolds number of 0.12×10^6/ft. Computational results for the Mach number and vorticity contours are presented to show the unsteady 3-D flow characteristics including shock waves and their interaction with boundary and shear layers. The computed SPL and turbulent kinetic energy spectra are also presented and the SPL variation along the cavity floor mid-span is compared to existing experimental data.

Methodology

Unsteady compressible viscous flow solutions for the Navier-Stokes equations in conservation law form were obtained using the WIND code[20]. WIND solves the time-dependent, RANS equations for turbulent, compressible flows using a cell-vertex, finite-volume, time-marching approach on structured grids. A variety of spatial discretization schemes, as well as, algebraic, one-equation, and two-equation turbulence models are available in WIND. In addition, two DES formulations, based on the Spalart-Allmaras and Menter SST models, have been incorporated in the code. In the present investigation, the simulations were conducted using the SST based DES model.

The solution domain for the L/D = 5 cavity is shown schematically in figure 1. It allowed the turbulent boundary layer to develop on the flat plate, which extended 3D upstream of the cavity's forward bulkhead. Free stream conditions were set for the supersonic inflow and first order extrapolation was applied at the upper boundary, which was at 3D above the cavity opening. First order extrapolation was also applied at the downstream boundary, 3D behind the rear bulkhead. The cavity width, W, was equal to 0.5D and periodic boundary conditions were applied in the span-wise direction.

The discretization of the solution domain was based on a RANS type grid with 205 _94 _ 40 grid points in the stream-wise, normal and span-wise directions. The grid was packed near the walls, with a minimum grid spacing of 1_10^{-3}D, to maintain $y^+ < 3$ for the first grid point and 15 grid points within the 0.1D boundary layer thickness at the upstream cavity lip. The aspect ratio in the grid varied between 1 and 5 in all three directions.

The solution domain was decomposed into three non-overlapping zones upstream, across and downstream of the cavity. The third order upwind-biased Roe scheme was used for spatial discretization with TVD operator to suppress the numerical instabilities in the shear layer and near the shock waves. Though the fifth order Roe scheme was available in the WIND code it was not used because the corresponding default zone coupling procedure was not available. The parallel computations for the three zones were performed using three clustered Linux machines.

Explicit time marching scheme with Newton like sub-iterations was used for temporal advancement. The DES simulations were initiated in the unsteady mode and continued over 200,000 constant time-steps of $4.2345 \_10^{-7}$ seconds. It took 100,000 time steps to purge out the transient flow and establish resonance and the remaining 100,000 time steps to compute 20 cycles.

Results and Discussions

The DES simulations were performed for Mach 1.19 flow over an L/D =5 cavity at a Reynolds number of $2 \_ 10^5$ based on the cavity length. Figure 2 presents sample Mach number contours at the cavity mid-span. The figures show that an oblique shock is formed upstream of the cavity with a subsequent increase in the incoming boundary layer thickness

due to shock interactions. The unsteadiness of the flow field can be deduced from the change in the Mach number contours with time.

Figures 3 and 4 show the corresponding mid span vorticity components in the span-wise and axial directions respectively. The roll up of the vortex and the impingement of the shear layer at the rear bulkhead can be seen in figure 3. The figures also indicate the formation of eddies that are smaller than the shed vortex within the cavity. The three-dimensionality of the flow field solution can be deduced from the contours of the axial component of vorticity in figure 4. Contours of the normal vorticity component on the cavity floor and the plane downstream of the cavity rear bulkhead, which are presented in figure 5, demonstrate the evolution of the three-dimensional flow within the cavity.

Figure 6 and 7 present the pressure fluctuations and the sound pressure level (SPL) spectra near the cavity front and rear bulkhead. The SPL spectra were calculated from the pressure fluctuations using 8192 sample points One can see that, in general, the pressure fluctuations are chaotic and the amplitude as well as the SPL is higher at the rear bulkhead. Figure 7 indicates that the SPL spectra have a broadband content with a wide range of frequency scales.

Figure 8 shows three instantaneous turbulent kinetic energy (TKE) profiles at mid-span near the cavity's front and rear bulkhead. One can see that the profiles exhibit significant kinetic energy content across the shear layer, and within the cavity beyond the front bulkhead. Figure 9 shows sample TKE spectra in the shear layer near the cavity's front and rear bulkhead. The spectra show a broad band content over a wide range of frequency.

URANS simulations were conducted using the same discretization grid and 3rd order upwind Roe scheme as in the DES simulations. WIND RANS simulations based on two and one equation turbulence models (SST and S-A) became steady for both 3D and 2D configurations. However, the WIND URANS simulations using the Baldwin-Lomax turbulence model resulted in unsteady flow solution (Table 1). Additional 2-D URANS simulations were performed using FDL2DI[21], the AFRL code developed by Gaitonde et al.[21], which also resulted in unsteady flow solution. The 3rd order Roe-scheme and Baldwin-Lomax turbulence model along with the Beam-Warming implicit time integration were used in the FDL2DI URANS simulations. That enabled a larger time step of 6×10^{-6} seconds compared to 4.2345 _10^{-7} seconds for the WIND code. Figure 10 presents the computed time history of the pressure fluctuations and the sound pressure level (SPL) spectra near the cavity front and rear bulkheads from the FDL2DI simulations, calculated using 65536 sample points. Comparing figures 6 and 10 one can observe that unlike the DES results, the URANS predicted pressure fluctuations are not chaotic and SPL spectra have tonal frequencies and little or no broadband content.

Figure 11 compares the computed overall SPL (OASPL) along the cavity floor to the experimental result of DERA[22] for L/D = 5.0 cavity at M=0.85 and Reynolds number of $4.07\text{x}10^6$/ft. Proper scaling was applied to the computed 3-D DES SPL which was based on fewer sample points than the 2D URANS SPL results. One can see that the experimental SPL mean value is 160 dB and that the SPL near the rear endwall is 15dB higher than the front endwall. The figure shows that both 3D SST based DES and 2D URANS predict the general rise in SPL towards the rear end wall, but are higher than the experimental value of the SPL by 5dB. However, the detailed SPL variation along the cavity floor is better predicted by DES.

Conclusions

Detached Eddy Simulations (DES) were performed for unsteady three-dimensional supersonic flow over an open L/D = 5 cavity at free-stream Mach number of 1.19. The presented results reveal the basic flow features, including the vortex shedding, shock waves, and coupling of the acoustic and vorticity fields. The presented vorticity contours demonstrate the three-dimensional flow characteristics. The computed SPL spectra had broad band content over a wide range of frequencies even though the SST based DES simulations did not predict a fully turbulent boundary layer at the simulated Reynolds number of 0.12×10^6/ft. The calculated SPL distribution over the cavity floor closely followed the experimentally measured variation. The computations over estimated the SPL by only 3-5 dB over most of the cavity floor including near the rear endwall. The study demonstrates that DES formulation is an effective method for performing unsteady simulations for cavity flow-fields at resources, which are moderately higher than those required for 3-D URANS simulations.

Acknowledgements

This research was supported by a DAGSI grant AFRL/VA-UC-00-01; Mr. M. Stanek and Dr. M Visbal, technical monitors. Computations involving

FDL2DI were performed in ORIGIN 2000 at the Ohio Super Computer center. The authors would like to thank Dr. D. V. Gaitonde and Dr. D. Rizzetta for their valuable suggestions regarding the FDL2DI code and Mr. Robert Ogden of UC for providing technical support.

References

1. Grace, S., "An overview of Computational Aeroacoustic Techniques applied to cavity noise prediction", AIAA Aerospace Sciences Meeting 2001, Reno NV, January, AIAA-2001-0510.
2. Shih S. H, Hamed, A, Yeuan J. J., "Unsteady Supersonic Cavity Flow Simulations Using Coupled Kappa-Epsilon and Navier-Stokes Equations", Oct 1994, AIAA Journal, Vol. 32, No. 10, pp. 2015-2021.
3. Rizzetta, D. P., "Numerical Simulations of Supersonic flow over a three-dimensional cavity", 1988, AIAA Journal, Vol. 26, No. 7, pp. 799-807.
4. Sinha, N., Dash, S. M., Chidambaram, N. and Findlay, D., "A Perspective on the Simulation of Cavity Aeroacosutics", 1998, AIAA-98-0286.
5. Colonius, T., Basu, A. J., and Rowley, C. W., "Numerical Investigation of the Flow Past a Cavity," 1999, AIAA 99-1912.
6. Hamed, A., Basu, D., Mohamed, A. and Das, K., "Direct Numerical Simulations of Unsteady Flow over Cavity," 2001, Proceedings 3rd AFOSR International Conference on DNS/LES (TAICDL), Arlington, Texas.
7. Rizzetta, D. P. and Visbal, M. R., "Large-Eddy Simulation of Supersonic Cavity Flowfields Including Flow Control", 2002, 32nd AIAA Fluid Dynamics Conference, AIAA-2002-2853.
8. Stanek, M. J., Raman, G., Kibens, V., Ross, J. A., Odedra, J., and Peto, J. W., "Control of Cavity Resonance Through very High Frequency Forcing", 2000, AIAA-2000-1905.
9. Arunajatesan, S., Shipman, J. D., and Sinha, N., "Hybrid RANS-LES simulation of cavity flow fields with control", 2002, AIAA-2002-1130.
10. Spalart, P. R., Jou, W. H., Strelets, M., and Allmaras, S. R., " Comments on the Feasibility of LES for Wings, and on a Hybrid RANS/LES Approach," ,1997, First AFOSR International Conference on DNS/LES, Ruston, Louisiana, USA.
11. Spalart, P. R., and Allmaras, S. R., " A one-equation turbulence model for aerodynamic flows", La Rech. A'reospatiale, 1994, Vol. 1, pp. 5-21.
12. Kumar, Satish and Loth, Eric, " Detached Eddy Simulations of an Iced-Airfoil",2001, 39th AIAA Aerospace Sciences Meeting and Exhibit, AIAA-2001-0678.
13. Shieh, C. M., and Morris, P. J., "Comparisons of Two- and Three-Dimensional Turbulent Shallow Cavity Flows", 2001, 39th AIAA Aerospace Sciences Meeting and Exhibit, AIAA -2001-0511.
14. Travin, A., Shur, M., Strelets, M. and Spalart, P. R., "Detached-Eddy Simulations Past a Circular Cylinder", 1999, Flow Turbulence and Combustion, Vol. 63, pp. 293-313.
15. Schmidt, Stefan, and Thiele, Frank, "Comparison of numerical methods applied to the flow over wall-mounted cubes", 2002, International Journal of Heat and Fluid Flow, Vol. 23, pp. 330-339.
16. Forsythe, J. R, Squires, K. D., Wurtzler, K. E., Spalart, P. R., "Detached-Eddy Simulation of Fighter Aircraft at High Alpha", 2002, AIAA-02-0591.
17. Bush, R. H., and Mani, Mori, "A two-equation large eddy stress model for high sub-grid shear", 2001, 31st AIAA Computational Fluid Dynamics Conference, AIAA-2001-2561.
18. Menter, F. R., "2-Equation Eddy-Viscosity Turbulence Models For Engineering Applications", 1994, AIAA Journal, Vol. 32, No. 5, pp. 1598-1605.
19. Strelets, M., "Detached Eddy Simulation of Massively Separated Flows", 2001, 39th AIAA Aerospace Sciences Meeting and Exhibit, AIAA-2001-0879.
20. http://www.grc.nasa.gov/www/wind
21. Gaitonde, D., and Visbal, M. R., "Further development of a Navier-Stokes Solution Procedures Based on High-Order Formulas," AIAA-1999-0557, 1999.
22. Ross, J. et al, "DERA Bedford Internal Report, MSSA CR980744/1.0', 1998.

Table 1: Summary of conducted numerical simulations

Simulation	Turbulence model	Code	Grid	Summary
3-D DES	SST based DES	WIND	205 _ 94 × 40	Broad band content over a wide range of frequency
2-D & 3-D URANS	SST	WIND	205 _ 94 _ 40	Solution became steady
2-D URANS	SST	WIND	205 x 94	Solution became steady
2-D URANS	Baldwin-Lomax	WIND	205 x 94	Unsteady flow with tonal frequencies
2-D URANS	Baldwin-Lomax	FDL2DI	205 x 94	Unsteady flow with tonal frequencies

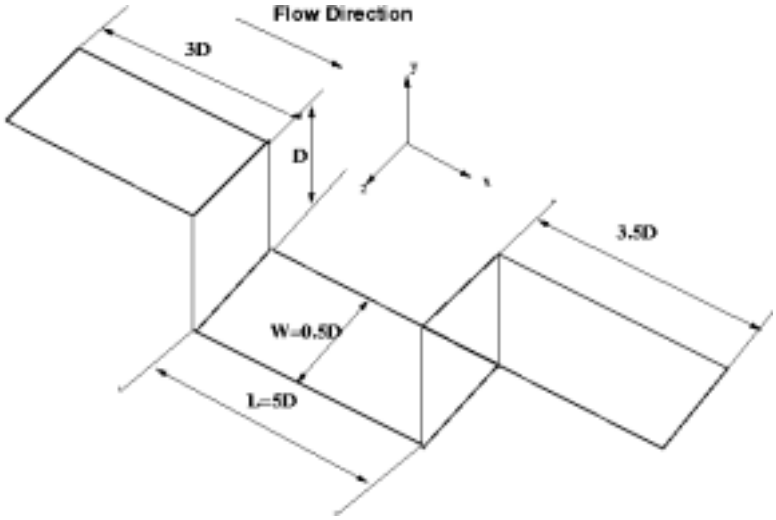

Figure 1 Schematic representation of the cavity configuration

T=T1 T=T2

Figure 2 Mach number contours at the cavity mid-span

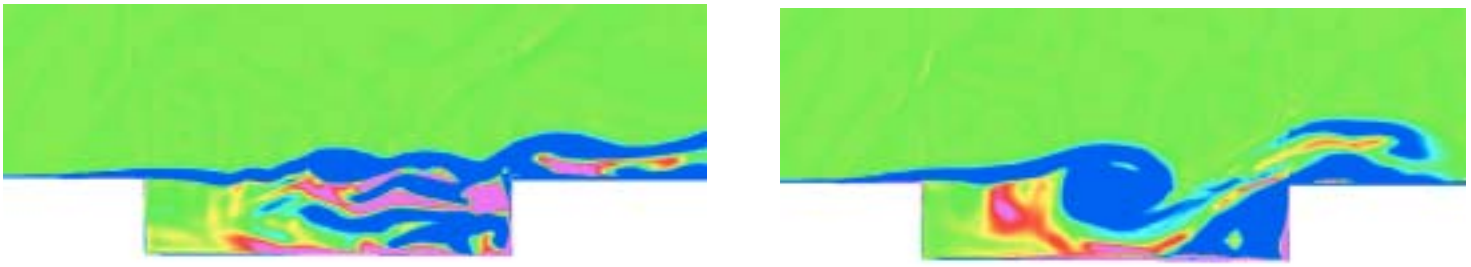

T=T1 T=T2

Figure 3 Span-wise vorticity component (ω_z) at cavity mid-span

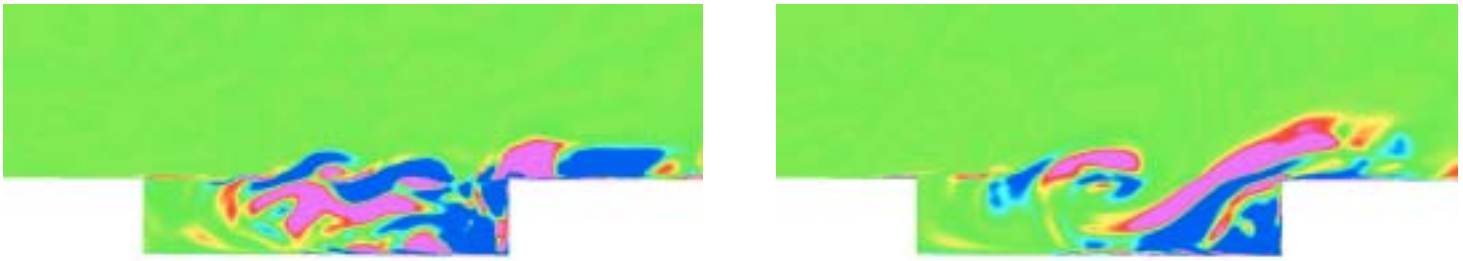

T=T1 T=T2

Figure 4 Axial vorticity component (ω_x) at cavity mid-span

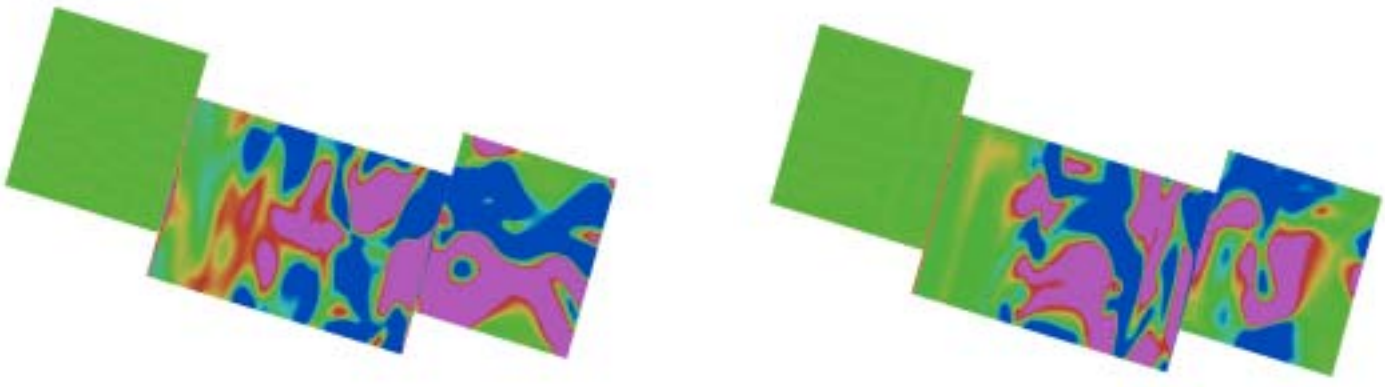

T=T1 T=T2

Figure 5 Normal vorticity component (ω_y) over cavity floor and downstream plane

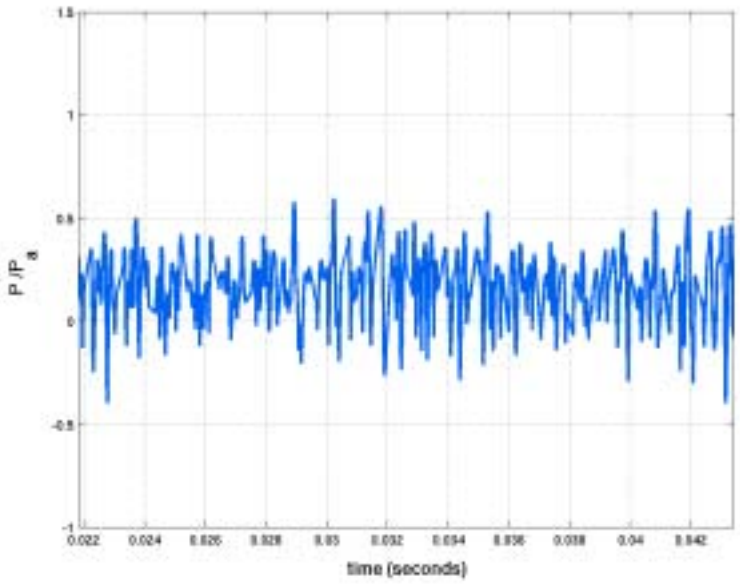

Near Front bulkhead

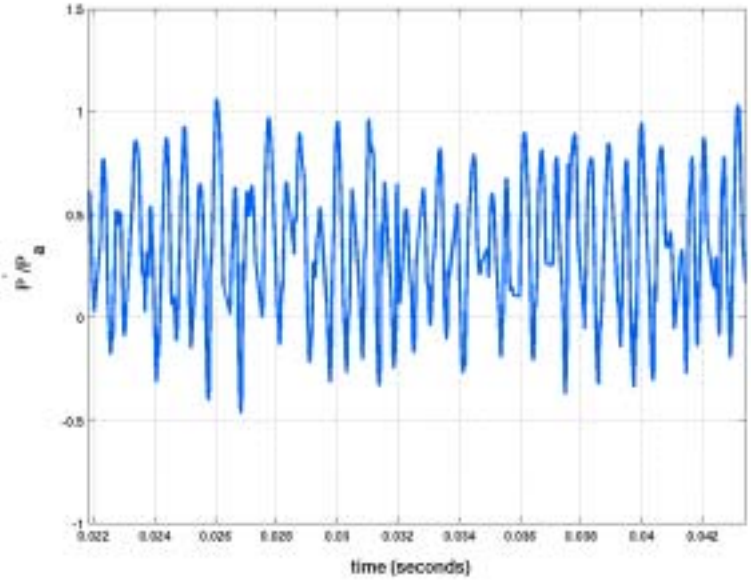

Near rear bulkhead

Figure 6 Pressure fluctuation history from 3-D DES

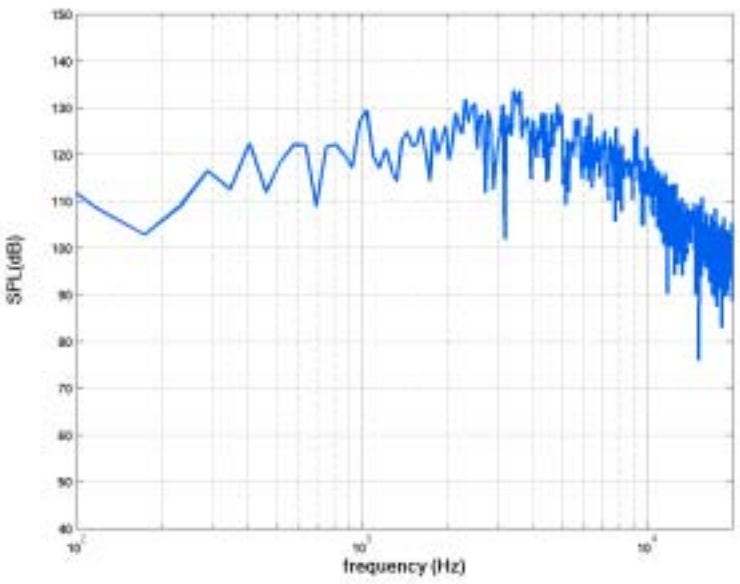

Near Front bulkhead

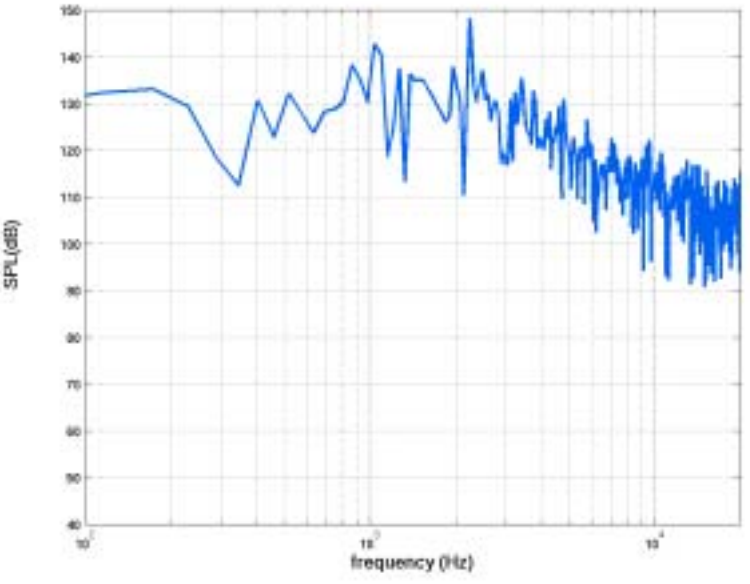

Near rear bulkhead

Figure 7 Sound pressure level spectra from 3-D DES (8192 sample points)

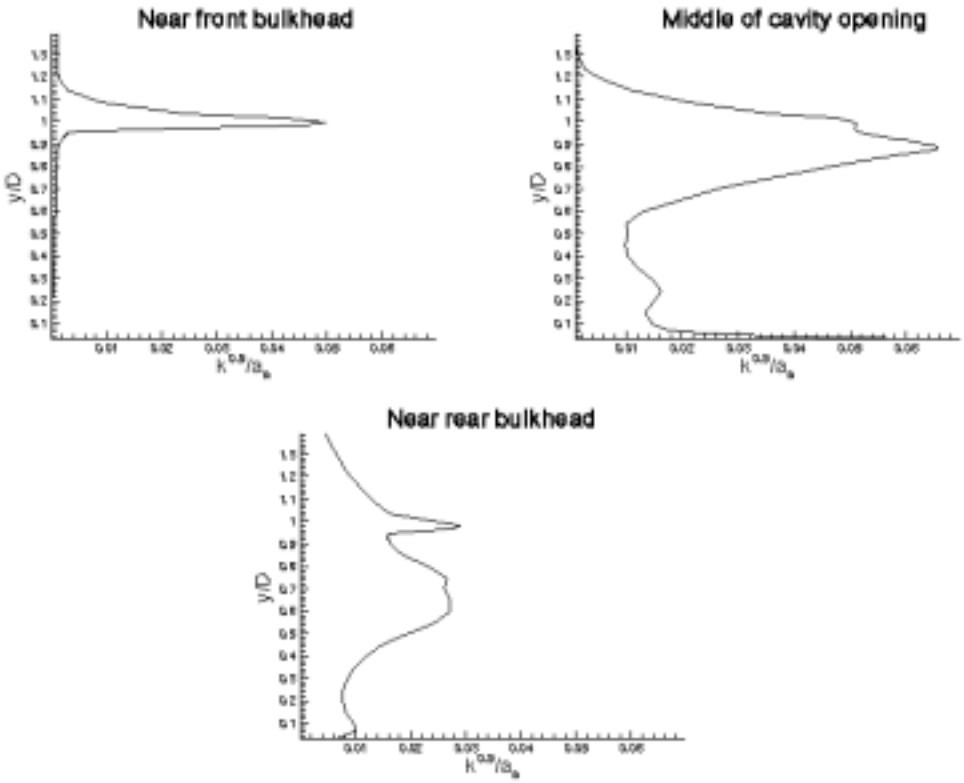

Figure 8 Kinetic energy profiles in the cavity shear layer

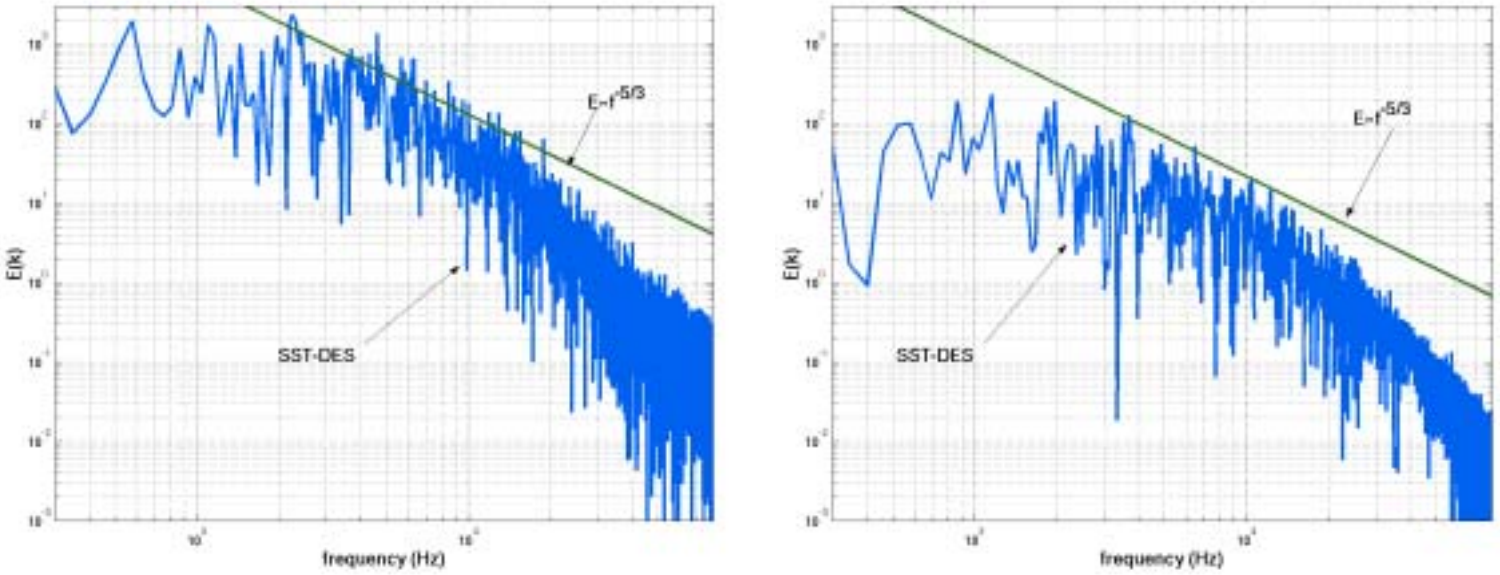

Near front bulkhead Near rear bulkhead

Figure 9 Turbulent kinetic energy spectra in the cavity shear layer

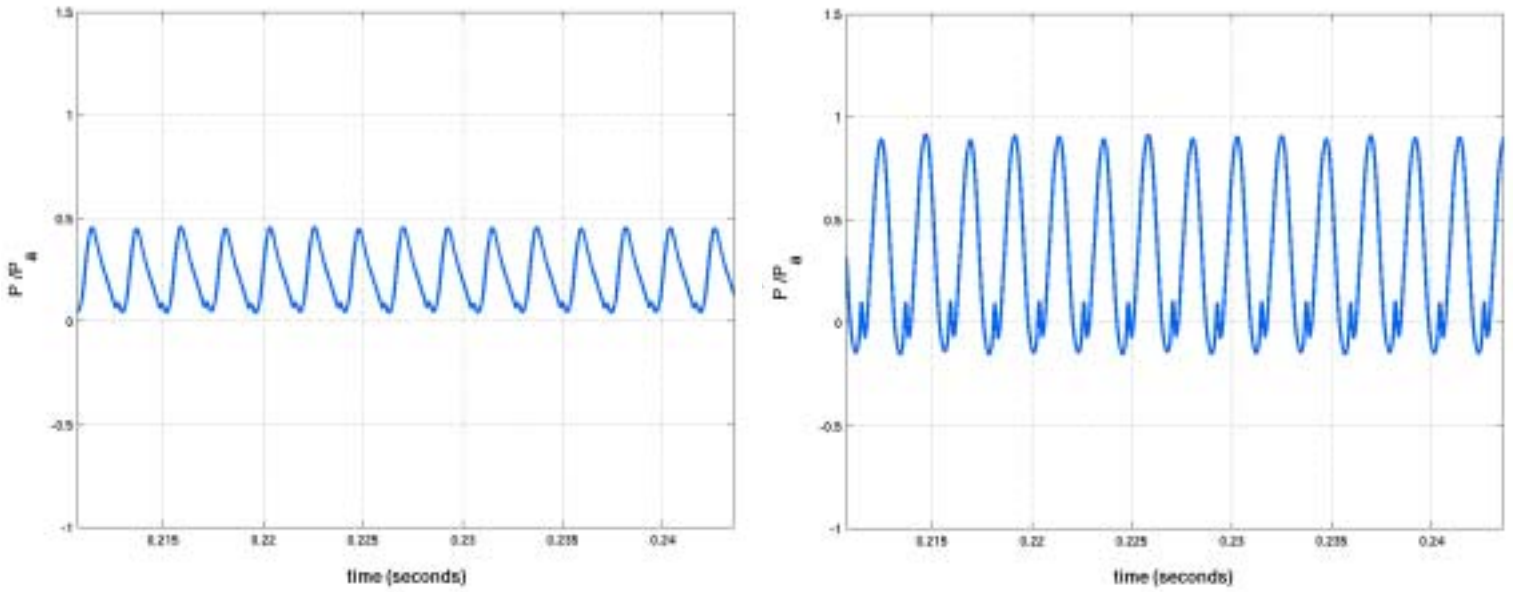

Near front bulkhead Near rear bulkhead

Figure 10(a) Pressure fluctuation history from FDL2DI

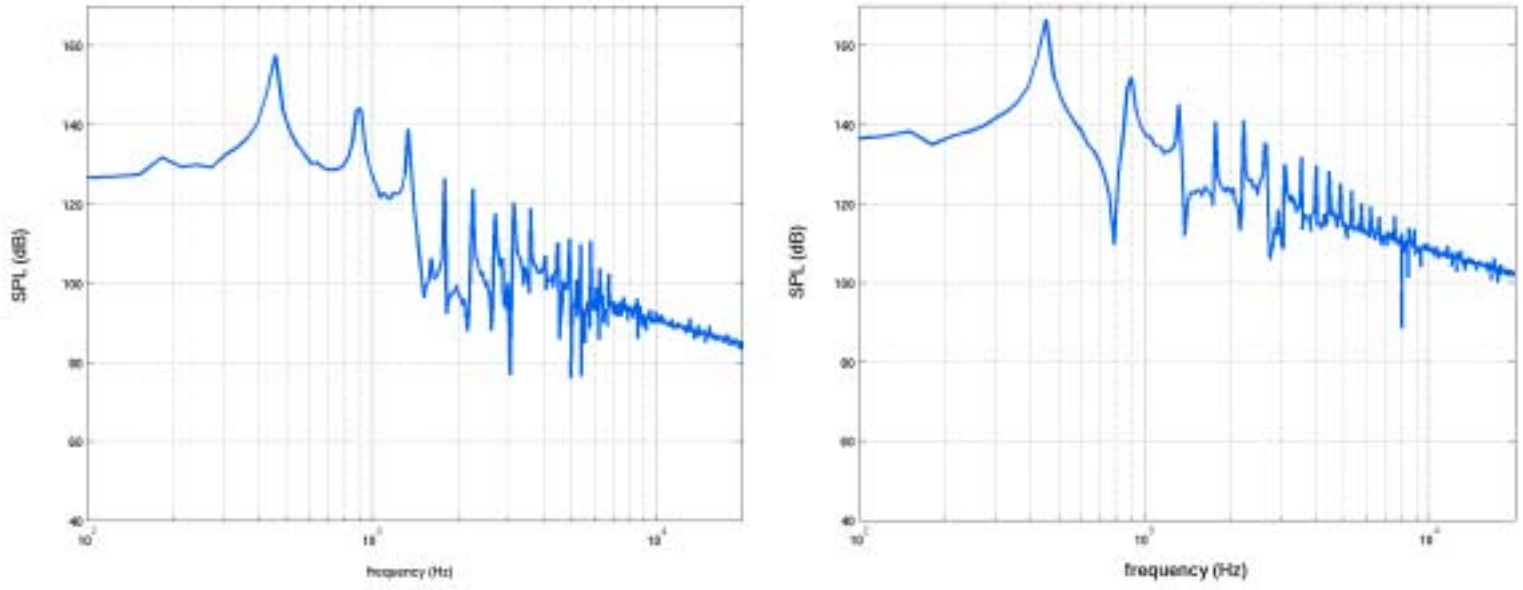

Near front bulkhead Near rear bulkhead

Figure 10 (b) Sound pressure level spectra from FDL2DI (65536 sample points)

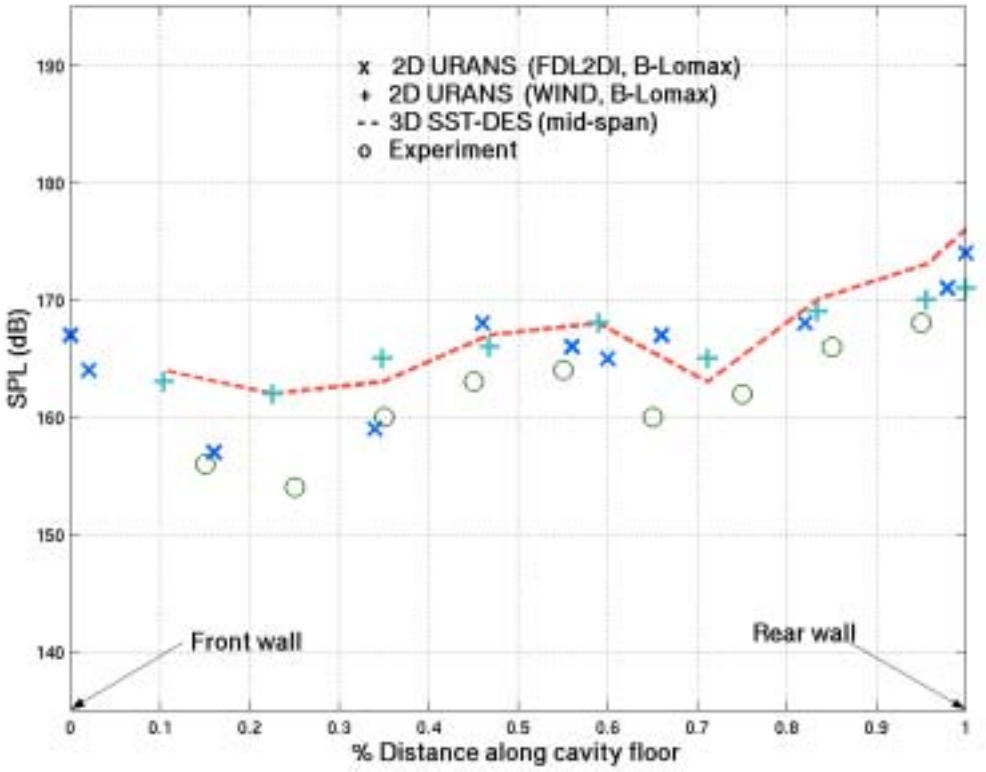

Figure 11 Variation of SPL along the cavity floor